Direct Observation of Localized Parallel Electric Fields in a Space Plasma

R. E. Ergun,* Y.-J. Su, and L. Andersson

The Laboratory for Atmospheric and Space Physics, University of Colorado, Boulder, Colorado 80309

C. W. Carlson, J. P. McFadden, and F. S. Mozer

Space Sciences Laboratory, University of California, Berkeley, California 94720

D. L. Newman and M. V. Goldman

The Center for Integrated Plasma Studies, University of Colorado, Boulder, Colorado 80309

R. J. Strangeway

Institute for Geophysical and Planetary Physics, University of California, Los Angeles, California 90055

We report direct measurements of parallel electric fields related to particle acceleration in a collisionless space plasma. The electric field is that of a monotonic potential ramp localized to ~10 debye lengths along the magnetic field. Electrons accelerated by the parallel electric field are accompanied by intense electrostatic waves and nonlinear structures interpreted as electron phase-space holes.

Visible auroral arcs are known to come from energetic (~10 keV) electrons that are accelerated earthward by magnetic-field-aligned (parallel) electric fields [1]. In this region, parallel electric fields ($E_\parallel$) arise from a combination of strong "upward" currents and a substantial magnetic mirror ratio (~400) between the source electron population in the tail of the Earth's magnetosphere and the visible arc in the ionosphere [2]. Direct observations of $E_\parallel$ in the upward current region have been reported [3]. There is no generally accepted theoretical description of these parallel electric fields. Treatments include weak double layers [4], strong double layers [5], anomalous resistivity [6], and parallel potentials associated with ion cyclotron waves [7]. Collisionless, localized, parallel electric fields also have been seen to develop in expanding plasmas in laboratory experiments [8].

The recent uncovering of antiearthward, energetic (up to several keV) electron fluxes carrying the "downward" current in the auroral zone and accelerated by parallel electric fields [9,10] has established a second region in space in which parallel electric fields form in a collisionless plasma. These parallel electric fields also are associated with field-aligned currents and are seen at the boundary between the cold, dense, ionospheric plasma ($T_e \sim 1$ eV, $n_e \sim 10^2 - 10^5$ cm^{-3}) and hot, tenuous, magnetospheric plasma ($T_e \sim 500$ eV, $n_e \sim 1$ cm^{-3}). Although parallel electric fields have been inferred from observations, there has been no direct observation in this region as of yet.

The purpose of this Letter is to put forth direct observations of parallel electric fields and accompanying electron distributions in the downward current region of the aurora. The measured $E_\parallel$ indicates a nearly monotonic potential ramp that extends ~10 debye lengths (λ_D) along the ambient magnetic field (**B**). The electron distributions are substantially modified by $E_\parallel$ and accompanying electrostatic emissions. The unaccelerated electron distribution, referred to here as the "source" distribution, has a dense, cold core and displays some heating and a drift. The accelerated distribution, also referred to as the "downstream" distribution, has a peak at an energy that is consistent with the parallel potential and shows substantial modification due to wave-particle interactions. Immediately downstream of the parallel electric field are intense, broadband quasielectrostatic emissions that are identified as a series of electron phase-space holes previously associated with parallel electric fields in this region [11] and studied in numerical simulations [12,13]. These data suggest that parallel electric fields are highly localized and are associated with the generation of electron phase-space holes.

The observations are from the Fast Auroral SnapshoT (FAST) satellite [14] which measures electromagnetic fields and charged particle distributions of the aurora. The FAST satellite is in a near-polar orbit (83° inclination) with a 350 km perigee and a 4175 km apogee. Instruments include electron and ion spectrographs and three-axis electric field and magnetic field instruments.

We briefly discuss the measurement of the $E_\parallel$ since it is critical to this Letter. The electric field instrument uses a set of 8-cm, high impedance spherical probes (Fig. 1) to measure the vector field. The electric field in the spin plane of the satellite is derived from long-baseline (56 and 29 m) dipoles which measure the instantaneous (independent of satellite spin phase) electric field in the spin plane of the satellite to ±10 mV/m given a plasma density (n_e) > 5 cm^{-3}. The third component is measured with far less accuracy (±200 mV/m with n_e > 5 cm^{-3}) because of the short baseline (4 m). The satellite is oriented so that the spin plane is often nearly coplanar, within 3° of the plane formed by **B** and the spacecraft velocity,
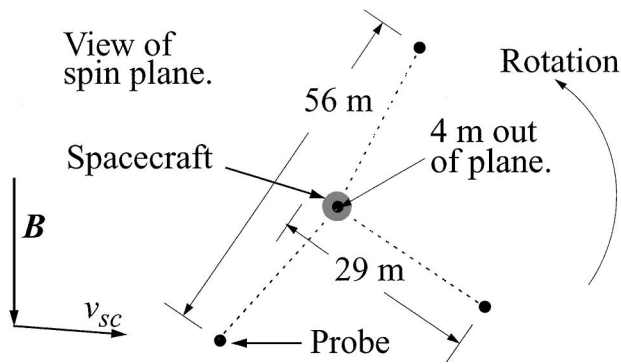
FIG. 1. Four probes form a tetrahedron that measures the vector electric field. The above sketch shows the approximate position at 15:35:0.5.10 UT (see later).

so the instantaneous $E_\parallel$ is measured with an accuracy of ± 20 mV/m if $n_e > 5$ cm^{-3}.

Figure 2 displays electric field and electron observations from the northern auroral zone. Figures 2a and 2b display, respectively, the dc to 100-Hz electric field perpendicular to **B** projected along the spacecraft path ($E_\perp$) and $E_\parallel$ ($\mathbf{E} \cdot \mathbf{B}/|\mathbf{B}|$). Figure 2c displays the antiearthward electron differential energy flux and Fig. 2d shows the broadband (1 to 16 kHz) electric field power.

$E_\perp$ (Fig. 2a) has a negative peak at $\sim$15:35:03 UT just as an antiearthward electron beam is seen (Fig. 2c). The
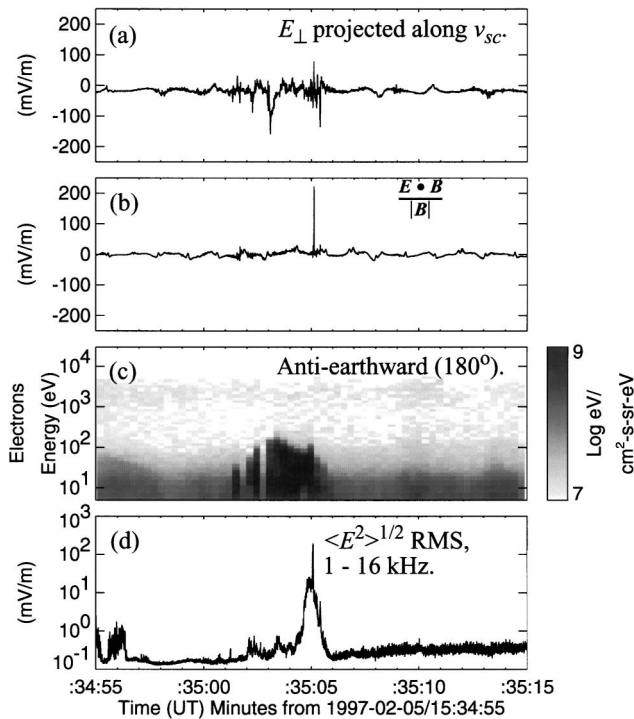

FIG. 2. (a) The electric field perpendicular to **B** and nearly along the spacecraft velocity. (b) $E_\parallel$. (c) The electron differential energy flux (shade) as a function of energy (vertical axis) and time (horizontal axis). The fluxes are integrated from 157.5° to 202.5° in pitch angle. (d) The omnidirectional wave electric field amplitude in the 1 to 16 kHz band.

signature is that of an electric field structure with positive divergence (Fig. 3) and interpreted as evidence of a downward parallel electric field on the magnetic flux tube of the electron beam [9,10] located earthward of the spacecraft until $\sim$15:35:05 UT. At that time, a large-amplitude, unipolar parallel electric field (Fig. 2b) is observed as the electron energy flux abruptly decreases (Fig. 2c). Intense wave emissions in the 1- to 16-kHz band (Fig. 2d) are seen just before the spacecraft detects the parallel electric field. Other than a hot ($\sim$2 keV), tenuous (1 cm^{-3}) magnetospheric population, ion fluxes (not displayed) are weak which indicates that the bulk energy is below the threshold of the detectors (<5 eV).

The geometry of the event is interpreted in Fig. 3. The spacecraft velocity ($\sim$5 km/s) was mostly perpendicular to **B**. The delay times between individual probes on the spacecraft (not displayed) is consistent with a structure (the region of parallel electric field) traveling antiearthward along **B** at a speed of 10 ± 5 km/s, near the estimated ion acoustic speed. Thus, the spacecraft crossed the parallel electric field from a region of accelerated electrons to the source region of unaccelerated electrons. The measured plasma properties are displayed in Tables I and II.

The measured $E_\parallel$ (Fig. 4a) indicates a nearly monotonic potential ramp. Given the relative spacecraft velocity of 10 ± 5 km/s, the ramp potential ($\Delta\Phi$) is 27 ± 13 V and the width of the ramp (10 ms) is $\sim$100 m, roughly $10\lambda_D$ using the accelerated electron parameters (Table I). The accelerated electron distribution shows a dramatic increase in fluxes peaking at $\xi = 35 \pm 4$ eV in energy over the source electron distribution (Fig. 4c). Within error,
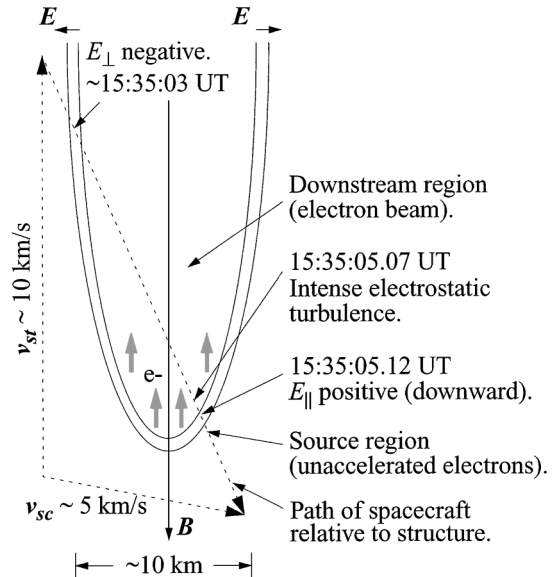

FIG. 3. The geometry of the observations in Fig. 2. The actual spacecraft velocity (v_{sc}) was nearly perpendicular to **B** at $\sim$5 km/s. The data are consistent with a potential structure moving $v_{\text{st}} \sim 10$ km/s in the $-\mathbf{B}$ direction (antiearthward), making an apparent spacecraft path as diagrammed.

TABLE I. Plasma parameters.

Parameter	Upstream	Accelerated	Uncertainty
λ_D	1.5 m	8.0 m	33%
ω_{pe}	$2\pi\ 7 \times 10^4$ s^{-1}	$2\pi\ 4 \times 10^4$ s^{-1}	33%
ω_{ce}	$2\pi\ 3.8 \times 10^5$ s^{-1}		<1%
ν_s (sound speed)	13 km/s	22 km/s	50%

$\xi = e\Delta\Phi$, lending strong support to the interpretation diagrammed in Fig. 3.

Langmuir probe measurements (not displayed) indicate that the source electron distribution has a dense ($n_e \sim 50$ cm^{-3}), cold ($T_e < 2$ eV) core (Table II), whereas the accelerated distributions have a significantly lower density. The source distribution, therefore, is dominated by a cold, dense core (which cannot be seen in Fig. 4c) but also has a heated population at ~ 6 eV. The accelerated electron distribution near the potential ramp is dominated by a population of electrons with $T_\parallel \sim 12$ eV and $T_\parallel/T_\perp \sim 6$. Further downstream from the parallel electric field, the electron distribution (not displayed) has no peak; rather, it appears as if heated and drifting. Throughout the region, there is a tenuous, ~ 1 cm^{-3}, hot, ~ 1.2 keV, electron population indicating a magnetic connection to the central plasma sheet in the magnetosphere. This population is not significantly perturbed by the parallel potential.

A sharp increase in wave power (Figs. 2d and 4b) accompanies the accelerated electrons ~ 400 m (40 ms) downstream of the potential ramp. The most intense wave power is seen for a ~ 50-ms period and has a relative energy density $W = \varepsilon_0 \mathbf{E}^2/2n_e T_e \cong 10^{-3}$ to 10^{-2} (ignoring the keV electrons of magnetospheric origin), a value which signifies strong modification of the electron distribution and possibly nonlinear behavior. The wave spectrum (Fig. 4d) shows intense, broadband, quasi-electrostatic emissions below the plasma frequency, a signature of propagating of electron phase-space holes [15]. No broadband (1–16 kHz) waveform data were transmitted during the above event; however, broadband waveform data from several similar events do reveal electron phase-space holes. Figure 5 displays the electric field waveform near the parallel electric field during another event which clearly shows the solitary structures.

Electron phase-space holes associated with parallel electric fields have been previously observed [11] and reported in numerical simulations [16]. Interestingly, electron phase-space holes produced in numerical simulations from bidirectional electron beams display evolved distributions similar to that in Fig. 4c [12,13]. These same numerical simulations and analytical investigations [17,18] predict whistler emission during the growth and evolution of electron phase-space holes. The wave electric field (Figs. 2d, 4b, and 4d) may also include whistler emissions.

A small survey of a FAST data set was conducted to verify the above event. The selected orbits were from active periods. $E_\parallel$, $\mathbf{E} \cdot \mathbf{B}/|\mathbf{B}|$, had to have a peak amplitude exceeding 10 times the rms amplitude averaged over a 10-s period surrounding the event. Once identified, the events were validated. The instrument must not have been saturated and none of the probes may have been on the flux tube connected to the spacecraft. Eight valid events were identified. All were on the boundary of a dramatic change in electron energy and seven of the eight indicate a monotonic potential ramp. During five of the events, high time resolution electric field waveforms were transmitted, all of which showed electron phase-space holes. The majority of the events appear in conjunction with Alfvén wave activity and/or intense wave turbulence and therefore are much more difficult to interpret unequivocally.

The direct observation of $E_\parallel$ is rare. There are several reasons that such events are expected to be infrequent. Spacecraft travel nearly perpendicular to $\mathbf{B}$ in the auroral region and $E_\parallel$ is confined to a thin layer along $\mathbf{B}$. If the structures are moving, such as the event above, the chance of being detected is much higher. However, remote sensing of electrostatic whistler waves from narrowly confined regions [19] indicates that the whistler sources are nearly stationary (<1 km/s) over a time period of tens of seconds. The motion in the above event (Figs. 2 and 3) may not be representative.

In the above event, the electron energy (~ 35 V) is small compared to observed energies of up to several kilovolts

TABLE II. Electron populations.

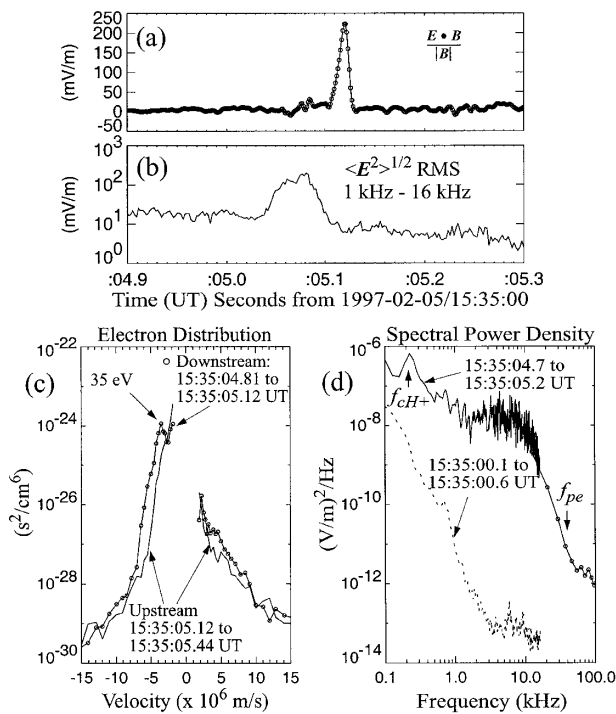| Electrons	n_e	T_e	ν_d
Upstream (cold)	50 ± 25 cm^{-3}	<2 eV	
Upstream (heated)	~ 5 cm^{-3}	~ 6 eV	$\sim 10^6$ m/s
Downstream (cold)	<5 cm^{-3}	<2 eV	
Downstream (accelerated)	12 ± 8 cm^{-3}	12 ± 3 eV (parallel) ~ 2 eV (perp.)	$\sim 2 \times 10^6$ m/s
Magnetospheric	0.9 ± 0.25 cm^{-3}	1200 ± 300 eV	~ 0

FIG. 4. (a) $E_\parallel$. (b) The rms electric field in the ~1- to 16-kHz band. Intense wave emissions are seen downstream of $E_\parallel$. (c) The circles represent the accelerated electron distribution at 0° and 180° pitch angles taken downstream of $E_\parallel$. A peak is at 3.5×10^6 m/s or 35 eV. The solid line is the unaccelerated electron distribution, upstream of $E_\parallel$. The distribution is drifting antiearthward. Further description is in Table II. (d) The electric field spectral power density downstream of $E_\parallel$ (solid line) and an earlier spectrum (dashed line).

[9]. Higher energy electron fluxes, in general, are seen with lower plasma densities and more intense wave emissions. Such conditions dramatically decrease the accuracy of the
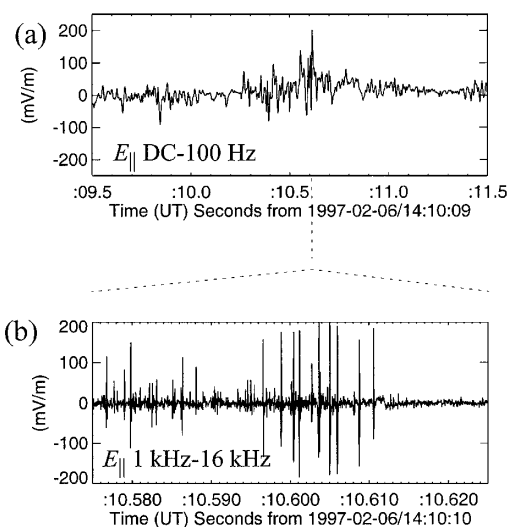
dc electric field instrument, reducing the probability of detecting the parallel electric field.

In summary, direct observations of $E_\parallel$ in the downward current region of the auroral zone indicate a potential ramp that extends ~$10\lambda_D$ along **B**. Intense quasielectrostatic wave emissions and electron phase-space holes appear to modify the accelerated electron distribution. These observations suggest that parallel electric fields are localized, e.g., [20], and are associated with the generation of large-amplitude electron phase-space holes and plasma waves.

FIG. 5. (a) dc $E_\parallel$ detected concurrently with up-going electron fluxes. (b) An expanded view of the wave electric field indicates solitary structures identified as electron phase-space holes.

[1] F. S. Mozer, C. W. Carlson, M. K. Hudson, R. B. Torbert, B. Parady, J. Yatteau, and M. C. Kelley, Phys. Rev. Lett. **38**, 292 (1977).
[2] S. Knight, Planet. Space Sci. **21**, 741 (1973).
[3] F. S. Mozer and C. A. Kletzing, Geophys. Res. Lett. **25**, 1629 (1998).
[4] M. Temerin, K. Cerny, W. Lotko, and F. S. Mozer, Phys. Rev. Lett. **48**, 1175 (1982).
[5] L. P. Block, Cosmic Electrodyn. **3**, 349 (1972).
[6] M. K. Hudson and F. S. Mozer, Geophys. Res. Lett. **5**, 131 (1978).
[7] S. Ishiguro, T. Sato, H. Takamaru, and The Complexity Simulation Group, Phys. Rev. Lett. **78**, 4761 (1997).
[8] G. Hairapetian and R. L. Stensel, Phys. Fluids B **3**, 899 (1991).
[9] C. W. Carlson, J. P. McFadden, R. E. Ergun, M. Temerin, W. Peria, F. S. Mozer, D. M. Klumpar, E. G. Shelly, W. K. Peterson, E. Moebius, R. Elphic, R. Strangeway, C. Cattell, and R. Pfaff, Geophys. Res. Lett. **25**, 2017 (1998).
[10] R. E. Ergun, C. W. Carlson, J. P. McFadden, F. S. Mozer, G. T. Delory, W. Peria, C. C. Chaston, M. Temerin, R. Elphic, R. Strangeway, R. Pfaff, C. A. Cattell, D. Klumpar, E. Shelly, W. Peterson, E. Moebius, and L. Kistler, Geophys. Res. Lett. **25**, 2025 (1998).
[11] R. E. Ergun, C. W. Carlson, J. P. McFadden, F. S. Mozer, L. Muschietti, and I. Roth, Phys. Rev. Lett. **81**, 826 (1998).
[12] M. V. Goldman, M. M. Oppenheim, and D. L. Newman, Geophys. Res. Lett. **26**, 1821 (1999).
[13] M. M. Oppenheim, D. L. Newman, and M. V. Goldman, Phys. Rev. Lett. **83**, 2344 (1999).
[14] C. W. Carlson, R. Pfaff, and J. G. Watzin, Geophys. Res. Lett. **25**, 2013 (1998).
[15] H. Matsumoto, H. Kojima, T. Miyatake, Y. Omura, M. Okada, I. Nagano, and M. Tsutsui, Geophys. Res. Lett. **21**, 2915 (1994).
[16] N. Singh, Geophys. Res. Lett. **27**, 927 (2000).
[17] D. L. Newman, M. V. Goldman, M. Spector, and F. Perez, Phys. Rev. Lett. **86**, 1239 (2001).
[18] Georgios Vetoulis and Meers Oppenheim, Phys. Rev. Lett. **86**, 1235 (2001).
[19] H. G. James, J. Geophys. Res. **81**, 501 (1976).
[20] H. Schamel and S. Bujarbarua, Phys. Fluids **26**, 190 (1983).